Osinga, H. M., & Hauser, J. (2005). The geometry of the solution set of nonlinear optimal control problems.

The geometry of the solution set of nonlinear optimal control problems

Hinke M. Osinga* and John Hauser†

November 28, 2005

Abstract

In an optimal control problem one seeks a time-varying input to a dynamical systems in order to stabilize a given target trajectory, such that a particular cost function is minimized. That is, for any initial condition, one tries to find a control that drives the point to this target trajectory in the cheapest way. We consider the inverted pendulum on a moving cart as an ideal example to investigate the solution structure of a nonlinear optimal control problem. Since the dimension of the pendulum system is small, it is possible to use illustrations that enhance the understanding of the geometry of the solution set. We are interested in the value function, that is, the optimal cost associated with each initial condition, as well as the control input that achieves this optimum. We consider different representations of the value function by including both globally and locally optimal solutions. Via Pontryagin's Maximum Principle, we can relate the optimal control inputs to trajectories on the smooth stable manifold of a Hamiltonian system. By combining the results we can make some firm statments regarding the existence and smoothness of the solution set.

Keywords: Hamilton-Jacobi-Bellman equation, Hamiltonian system, optimal control, Pontryagin's maximum principle, global stable manifolds

AMS subject classifications: 49J40, 49K20, 49L20, 53D12, 65P10

*Corresponding author: ++44 117 928-7600, Department of Engineering Mathematics, University of Bristol, Bristol BS8 1TR, UK (h.m.osinga@bristol.ac.uk).

†Department of Electrical and Computer Engineering, University of Colorado at Boulder, Boulder, CO 80309-0425, USA.

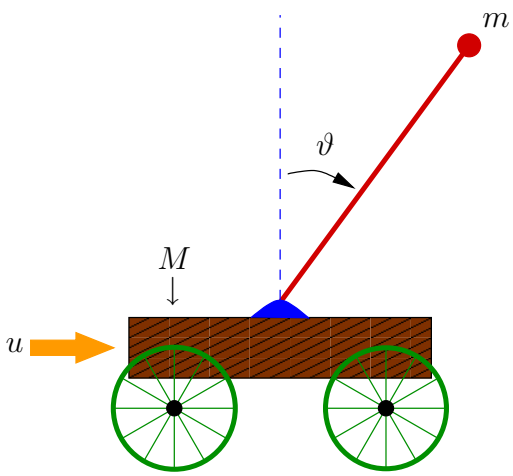

Figure 1: Sketch of the balanced planar pendulum on a moving cart.

1 Motivation

It is still an open question, in general, how to characterize the solution structure of nonlinear optimal control problems. A simple illustration of why this is so hard can be given with the problem of balancing an inverted (planar) pendulum on a moving cart. The situation is sketched in Fig. 1, where the mass of the pendulum is m, the mass of the cart M, the applied horizontal force u, and the offset angle from the vertical up position is ϑ; the equations are given in (1) below. We assume that the system is subject to a quadratic incremental cost function penalizing both the state and control, which we wish to minimize. For certain intial conditions, it is not hard to describe the optimal control action: if the pendulum is in a downswing only a little bit off the vertical up position, we counteract this motion by moving the cart under the center of gravity. Since the offset is small, that is, the penalty on the state is small, and since this control action achieves its goal quickly, the total cost will be optimal. However, if the pendulum is in the downswing quite far away from the vertical up position, it will be cheaper to wait and watch the pendulum pass the vertical down position. Only as it swings back, when the pendulum is in the upswing, one "catches" it. Here, the cost increment of the longer duration of the control action outweighs the size of the penalty incurred when counteracting the downswing motion. Hence, somewhere in between there must be intial conditions where the cost is the same whether we counteract the downswing, or whether

we wait and control the upswing. However, this means that this simple optimal control problem does not even have a uniquely defined minimizing control action for arbitrary, and quite "normal" initial conditions! From a control theoretic point of view this seems to indicate that there is no hope of getting smooth minizing control functions, let alone proper feedback laws that depend smoothly on the initial conditions. This paper shows that the situation is not so bad and that, under mild assumptions, much of the regularity and smoothness is preserved.

The class of control problems for which our statements hold is introduced in Section 2. We use the example of the inverted pendulum on a moving cart to illustrate the nature of this class of problems. We wish to understand how the optimal cost depends on the initial conditions, that is, whether the so-called *value function* is continuous and what we can say about its smoothness.

There are two different approaches to optimal control problems, namely so-called *dynamic programming* and *variational methods*; see Sontag [Sontag, 1998, chapter 8]. We shall take a geometric point of view and discuss both methods in the context of the inverted pendulum example. We generalize the results obtained by Lukes [1969] who studied this problem locally in a neighborhood where the optimal controls are unique.

This paper is organized as follows. In the next section we properly define the problem of balancing the inverted pendulum on a moving cart and characterize the class of problems for which our results hold. Section 3 gives a brief overview of the results for so-called linear quadratic (LQ) optimal control problems. These are the simplest optimal control problems and can be solved explicitly. The general problem of nonlinear optimal control is then analyzed further. Section 4 explains the dynamic programming methods and provides an overview of the theory in this context. The same is then done for the variational approach in Section 5. Both sections contain illustrations showing the geometric structure of the solutions for the inverted pendulum. We compare the two methods in Section 6 and summarize the results in Section 7.

2 Problem formulation

The example of the inverted pendulum on a moving cart is quite simple, and it helps to understand the nature of nonlinear optimal control problems in general, as it shows what should be expected as typical in the nonlinear case. Moreover, the dimensions are such that it is relatively easy to visualize the behavior. This example was also used in [Hauser and Osinga, 2001], [Jadbabaie *et al.*, 2001], and

[Jadbabaie *et al.*, 1999].

The pendulum is planar and the cart moves under an applied horizontal force u, constituting the control, in a direction that lies in the plane of motion of the pendulum; see also Fig. 1. The cart has mass M, the pendulum has mass m and the center of mass lies at distance l from the pivot (half the length of the pendulum). The position of the pendulum is measured relative to the position of the cart as the offset angle ϑ from the vertical up position. The equations of motion can be derived from first principles, where we assume that there is no friction. Furthermore, we ignore the cart and only consider the equations associated with the pendulum. Writing $x_1 = \vartheta$ for the angle, and $x_2 = \dot{\vartheta}$ for the angular velocity, the equations are

$$\left\{ \begin{array}{rcl} \dot{x}_1 & = & x_2 \\ \dot{x}_2 & = & \dfrac{\frac{g}{l}\,\sin(x_1) - \frac{1}{2}\,m_r\,x_2^2\,\sin(2x_1) - \frac{m_r}{ml}\,\cos(x_1)\,u}{\frac{4}{3} - m_r\,\cos^2(x_1)}, \end{array} \right. \tag{1}$$

where $m_r = \frac{m}{m+M}$ is the mass ratio. We take the plane $\mathbb{R}^2$ as the state space of this system, rather than the cylinder $\mathbb{R}/(2\pi\mathbb{Z}) \times \mathbb{R}$, and the origin corresponds to the vertical up position of the pendulum. Throughout this paper, we use the parameter values $m = 2\,\mathrm{kg}$, $M = 8\,\mathrm{kg}$, $l = 0.5\,\mathrm{m}$, and $g = 9.8\,\mathrm{m/s^2}$.

As mentioned in the introduction, we assume that the control of (1) incurs a cost penalizing both the state and the control. That is, given an initial condition x_0 and an appropriate control action $u(\cdot)$ that balances the pendulum, the total cost is

$$J_\infty(x_0, u(\cdot)) = \int_0^\infty q(x^u(t), u(t))\,dt,$$

where $x^u(t)$ is the flow of the vector field (1) using the control $u(\cdot)$, with $x(0) = x_0$. Here, $q : \mathbb{R}^n \times \mathbb{R}^m \to \mathbb{R}$ is the incremental cost, which for the inverted pendulum is taken as a pure quadratic

$$q(x, u) = q_1 x_1^2 + q_2 x_2^2 + r u^2, \tag{2}$$

where $q_1 = 0.1$, $q_2 = 0.05$, and $r = 0.01$ throughout.

Given an initial condition $x_0 = (x_1(0), x_2(0))$, the goal is to get the pendulum in the vertical-up position, $(x_1, x_2) = (0, 0)$, while minimizing $J_\infty(x_0, \cdot)$. For convenience, we forget about the fact that the cart could be moving with large speed as we achieve this goal. Note that there is a symmetry in this problem: if $(x_1(t), x_2(t), u(t))$ is a solution, then so is $(-x_1(t), -x_2(t), -u(t))$ and $J_\infty(x_0, u(\cdot)) = J_\infty(-x_0, -u(\cdot))$.

2.1 General problem formulation

The results in this paper hold for more general optimal control problems. For example, system (1) is affine in u, but this is not a necessary condition. Also, the incremental cost need not be a pure quadratic. In general, we formulate the problem as follows. We wish to stabilize the origin of the system

$$\dot{x} = f(x(t), u(t)), \tag{3}$$

where $f : \mathbb{R}^n \times \mathbb{R}^m \to \mathbb{R}^n$ is C^2 and $f(0,0) = 0$. We assume linear controllability at the origin, that is, the augmented matrix $[B\ A\,B\ A^2\,B\ \ldots\ A^n\,B]$, formed by the matrices $A := D_x f(0,0)$ and $B := D_u f(0,0)$, has full rank.

The control action incurs an incremental cost $q : \mathbb{R}^n \times \mathbb{R}^m \to \mathbb{R}$ that fully penalizes both state and control. We assume that the incremental cost function is C^2 and quadratically positive definite; that is, there exists $c_q > 0$ such that

$$q(x,u) \geq c_q \left(\| x \|^2 + \| u \|^2 \right).$$

The total cost to be optimized is then

$$J_\infty(x_0, u(\cdot)) = \int_0^\infty q(x^u(t), u(t))\, dt,$$

as before, but $x^u(t)$ is now the solution of (3) with $x(0) = x_0$.

There is only *one* further assumption that we make for the results in this paper, namely that there exists a C^1 map $u^* = u^*(x,p)$ which globally minimises the pre-Hamiltonian

$$K(x,p,u) := q(x,u) + p^T f(x,u), \tag{4}$$

where $p \in \mathbb{R}^n$ and p^T means the transpose of p. Note that this assumption holds trivially for affine functions f as in (1) and quadratic q.

We are interested in the value function

$$V : x_0 \mapsto \inf_{u(\cdot)} J_\infty(x_0, u(\cdot)), \tag{5}$$

which relates the optimal cost with initial conditions x_0. Obviously, this optimal value function V is not defined for initial conditions x_0 that cannot be driven to the origin. Hence, the domain of V is that part of $\mathbb{R}^n$ which is stabilizable. Note that V could be infinite. For the inverted pendulum, the domain of V is $\mathbb{R}^n$, because this system is completely stabilizable, and V is finite for all $x_0 \in \mathbb{R}^n$.

It can be shown that the infimum in (5) for the general problem is, in fact, a minimum, because the optimal cost is attained for all x in the domain of V. The proof is similar to the proof in [Lee and Markus, 1967, Chapter 4] for Theorem 8 and uses direct methods of the calculus of variations; see [Buttazzo *et al.*, 1998] and [Dacorogna, 1989], and see also [Hauser and Osinga, 2001] for an outline of the proof. The assumptions that we use may be weakened; see for example [Hauser and Osinga, 2001] and [Cesari, 1983]. With the above assumptions the arguments in Proposition 3.1 of [Bardi and Capuzzo-Dolcetta, 1997] can be used to show that V is continuous on its domain.

3 The linear-quadratic problem

Let us first consider the linear-quadratic (LQ) problem; see also [Sontag, 1998]. Here, the state $x \in \mathbb{R}^n$ satisfies the linear equation

$$\dot{x} = Ax + Bu,$$

where (A, B) is controllable, and the incremental cost is written as

$$q(x, u) = \frac{1}{2}\left(x^T Q x + u^T R u\right),$$

with $Q, R > 0$. If one linearizes the general problem given in Section 2.1, then $A := D_x f(0,0)$, $B := D_u f(0,0)$, $Q := D_x^2 q(0,0)$ and $R := D_u^2 q(0,0)$.

The minimal cost for the LQ problem is then given by the optimal value function

$$V_L(x) := \frac{1}{2} x^T P x, \tag{6}$$

where P is the (unique) positive definite matrix that satisfies the algebraic Riccati equation

$$PBR^{-1}B^T P - PA - A^T P - Q = 0. \tag{7}$$

The optimal control that achieves this cost is unique and defined in feedback form by

$$u^* = -R^{-1}B^T P x.$$

Hence, the LQ problem has a globally well-defined unique solution and the optimal value function is smooth everywhere.

In the example of the inverted pendulum, the linearized system is

$$\dot{x} = \begin{bmatrix} 0 & 1 \\ \frac{g}{l(\frac{4}{3}-m_r)} & 0 \end{bmatrix} x + \begin{bmatrix} 0 \\ \frac{m_r}{ml(\frac{4}{3}-m_r)} \end{bmatrix} u,$$

with matrices

$$Q = \begin{bmatrix} 2q_1 & 0 \\ 0 & 2q_2 \end{bmatrix} \quad \text{and} \quad R = [2r]$$

for the incremental cost fuction. The solution of the algebraic Riccati equation (7) is then, approximately

$$P \approx \begin{bmatrix} 92.5409 & 22.2191 \\ 22.2191 & 5.3482 \end{bmatrix}.$$

The level sets of the associated value function V_L are ellipses with axes aligned along the eigendirections. The ratio between the axes of each ellipse is determined by the ratio of the eigenvalues of P. Since for the inverted pendulum this ratio is of the order 10^4, the ellipses are extremely elongated.

A visualization of the level sets is shown in Figure 2 for the range $[-1.5, 1.5] \times [-1.5, 1.5]$ in the (x_1, x_2)-plane. Low cost is blue, high cost is red, and the colors change linearly with the square root of the value function. The level sets are only shown up to $V_L = 10.89$.

4 Dynamic programming: the Hamilton-Jacobi-Bellman equation

When considering a nonlinear optimal control problem, one has to resort to numerical techniques. As mentioned in the introduction, there are two main approaches and the method of dynamic programming is the most straightforward to implement. The essence of dynamic programming is to treat the global problem as a concatenation of local problems. One first finds the optimal control, and thus the minimal cost, for initial conditions in a small neighborhood of the origin. In fact, the solution of the LQ problem can be used as an approximation that is valid on a small enough neighborhood. These local results are then used to find the minimal cost on a larger neighborhood, which can be repeated to enlarge the neighborhood further and further.

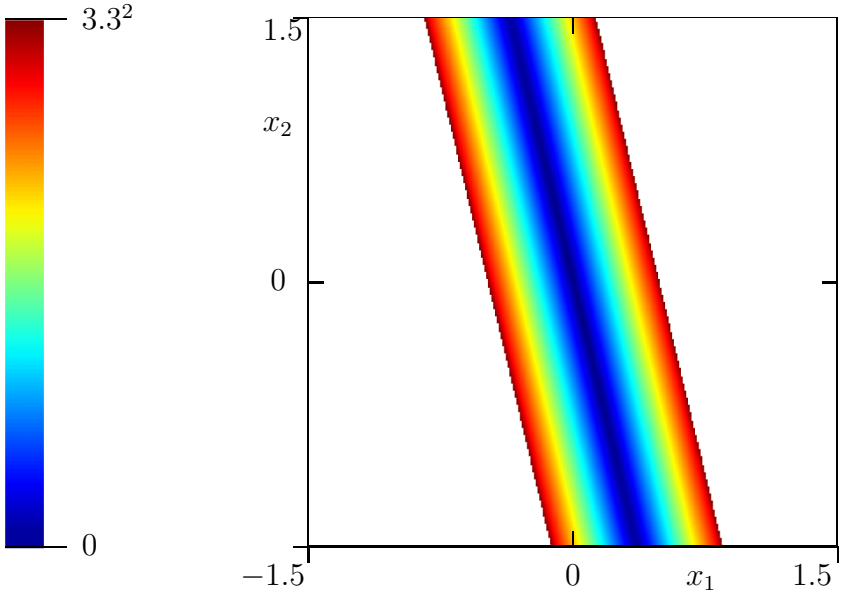

Figure 2: *The value function of the linearized system for* $x_1, x_2 \in [-1.5, 1.5]$. *Each point is colored in accordance with the color bar on the left indicating the associated optimal cost. No cost has been assigned to initial conditions with minimal cost higher than* 10.89.

More precisely, suppose V is known on a neighborhood Ω of the origin. Then we can enlarge the domain of V by considering all points x_0 that can reach Ω after a finite time T using a (locally) optimal control strategy. This is known as the finite-horizon approach; see [Jadbabaie *et al.*, 2001] and [Jadbabaie *et al.*, 1999]. Just outside Ω the value function satisfies

$$V(x_0) = J(T, x_0) := \min_{u(\cdot)} \int_0^T q(x^u(t), u(t))\, dt + V(x^u(T)).$$

Assuming differentiability of $J(T, x_0)$, we can formulate this as a partial differential equation, the so-called Hamilton-Jacobi-Bellman (HJB) equation

$$\left\{ \begin{array}{rcl} \dfrac{\partial}{\partial t} J(t,x) & = & -\min\limits_{u(\cdot)} \left[q(x,u) + \dfrac{\partial}{\partial x} J(t,x)\, f(x(t), u(t)) \right], \\ J(T,x) & = & V(x). \end{array} \right. \tag{8}$$

We refer to [Sontag, 1998] as a general reference and [Hauser and Osinga, 2001] for details on the proofs.

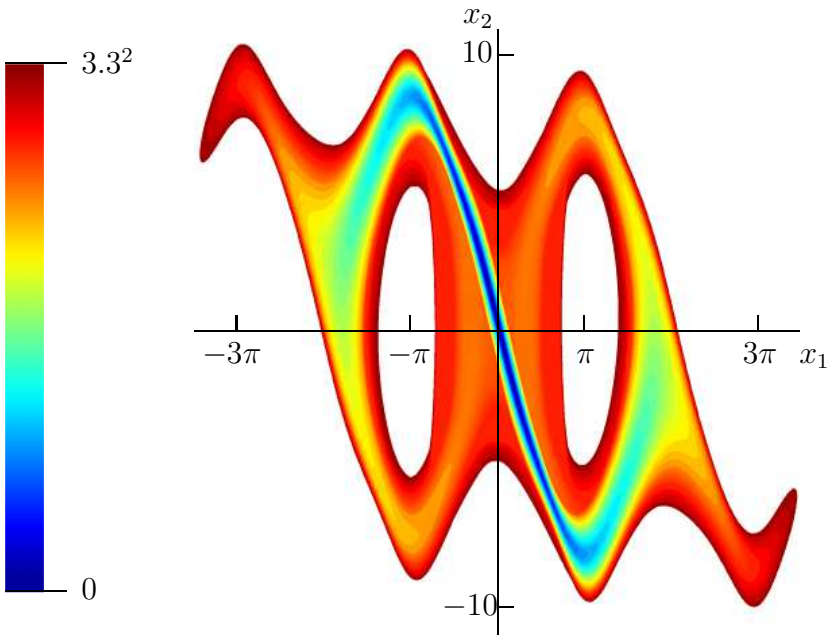

Figure 3: *The value function of the inverted pendulum for* $(x_1, x_2) \in [-11, 11] \times [-11, 11]$ *with minimal cost no higher than* 10.89*. Each point is colored in accordance with the color bar on the left indicating the associated optimal cost. See also the animation in the multimedia supplement [Osinga and Hauser, 2005].*

Figure 3 shows how the value function V depends on the initial conditions; see also the associated animation in [Osinga and Hauser, 2005]. Each initial condition $x_0 \in [-11, 11] \times [-11, 11] \subset \mathbb{R}^2$ is colored according to the value of V at x_0. Blue corresponds to low cost and red to high cost. The colors are assigned proportional to the square root of the value function up to a maximum of 10.89. Initial conditions with optimal costs higher than that are left blank. The picture clearly shows how the blue lowest cost corresponds to initial conditions where the pendulum has an offset but is on its way up. In contrast, if the pendulum is moving down, already a small deviation leads to a dramatic increase of the cost. This figure should be compared with the LQ solution of the linearized problem in Figure 2. Note that Figure 2 displays only a small square compared to Figure 3.

The similarity of Figure 2 and the corresponding part of Figure 3 is not a coincidence. Indeed, from a dynamical systems point of view, one would expect

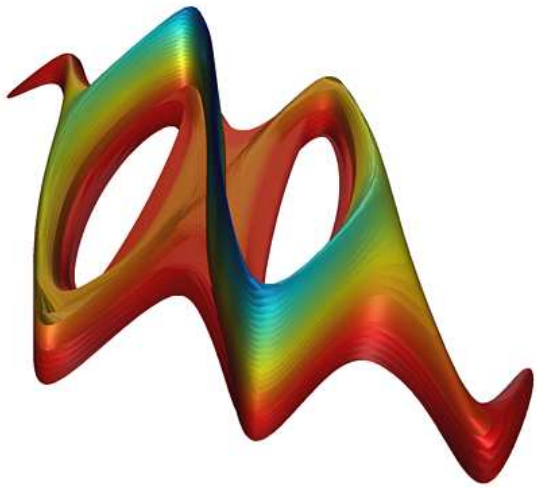

Figure 4: *The graph of the value function V for the inverted pendulum. The color coding is as in Figure 3. The view is along the negative V-axis; see also the animation in the multimedia supplement [Osinga and Hauser, 2005].*

that near the origin the value function of the nonlinear problem is tangent to the value function of the associated linear problem, and that smoothness and uniqueness of solutions to the linear problem carry over, at least locally, to the nonlinear problem. Lukes already showed in 1969 that this is true [Lukes, 1969].

We get a better idea of how V depends on $x = (x_1, x_2)$ by considering its graph in $\mathbb{R}^3$, which is depicted in Figure 4 with a view along the negative V-axis. This figure shows that V is continuous, but lacks differentiability for certain values of x; in particular, this can be seen in the associated animation in the multimedia supplement [Osinga and Hauser, 2005]. In fact, we show in [Hauser and Osinga, 2001] that, for our general class of systems, V is continuous and finite everywhere on its domain.

Even though we cannot think of the graph of V as a manifold, there is more to say about the local smoothness of this object. We computed V using the finite-horizon technique in combination with finding the direction of "steepest descent" to achieve local optimality. Effectively, successive enlargements of the domain on which V is known are determined by taking second-order approximations of the HJB equation (8) with infinitesimally small timestep T. These locally optimal

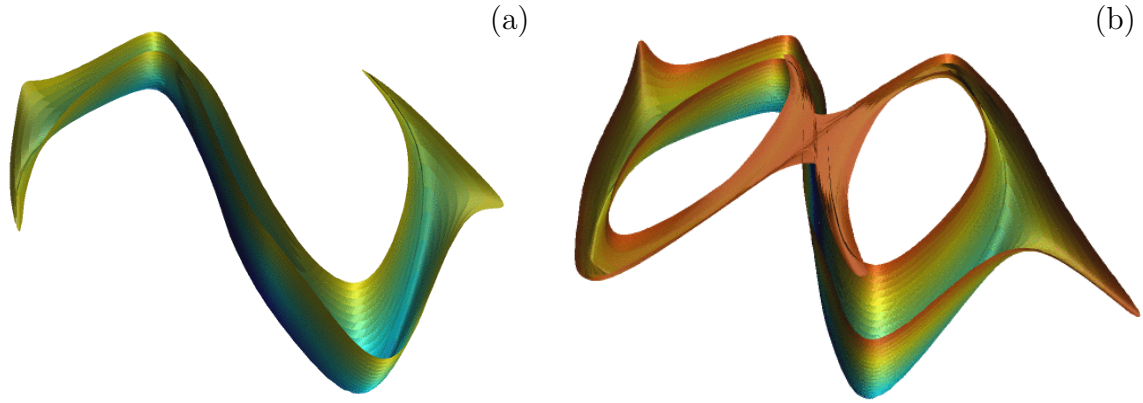

Figure 5: *The (locally) optimal level sets of the multi-valued function associated with V. The color coding is as in Figure 3. (a) Level sets up to 4.84; these are all both locally and globally optimal. (b) Level sets up to 6.8644; the onset of self-intersections. The animations in the multimedia supplement [Osinga and Hauser, 2005] show these objects from different points of view.*

solutions can be found directly from solving an algebraic Riccati equation. Our technique not only gives the globally optimal solutions, but control strategies may be chosen that are only locally optimal. We devised a continuation scheme following V, or rather a more complicated multi-valued function which includes the suboptimal solutions.

The isoclines of this multi-valued object are connected closed curves for all values of the cost. Figure 5 shows the first couple of isoclines. Initially, roughly up to $V = 6$, each isocline consists only of globally optimal solutions. The level sets are topological circles and the surface is topologically a paraboloid; see also Figure 6(a). As we consider higher level sets the topological circles curl so much that at some point an isocline reconnects with itself forming topologically a "triple figure-8" shape (the fact that there is a double tangency is due to the symmetry in the system). For even higher values the isoclines self-intersect. Only the outer contours are globally optimal solutions and additional suboptimal solutions form the closed connected self-intersecting curve. Figure 6 shows the deformation from

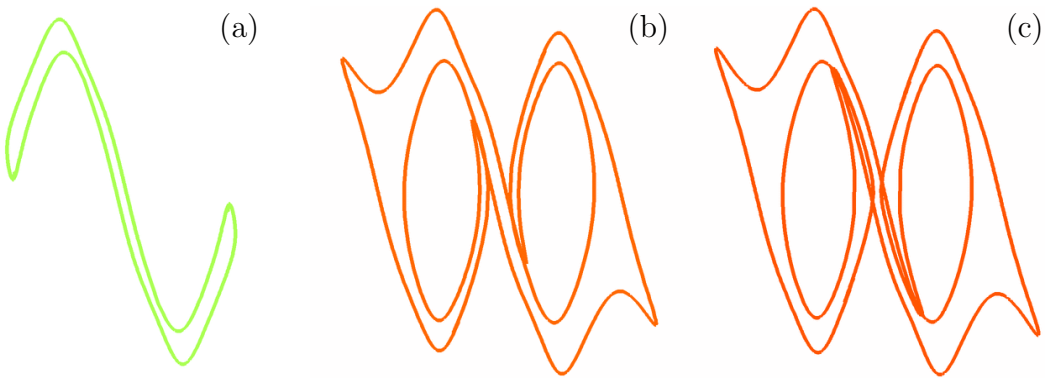

Figure 6: *Three isoclines of the multi-valued function associated with V. Isoclines deform from a topological circle containing only globally optimal solutions at level* 3.24 *(a), via a "triple figure-8" shape approximately at* 6.5536 *(b), into a self-intersecting set at level* 6.8644 *including locally optimal solutions as well.*

a topological circle at level 3.24, through a (double) tangency approximately at 6.5536, into a self-intersecting isocline at 6.8644.

The points of self-intersection form two smooth curves that act as ridges along which the value function V is not differentiable. Locally, away from these ridges, the value function is differentiable and even in a neighborhood of a ridge, we can think of the value function as switching between two differentiable functions. Except for those two curves, V is differentiable everywhere. Further along, for higher values of V, level sets reconnect and subsequently self-intersect again, creating more intersection points. Certainly in the area we explored (including filling up the holes around the hanging down solution $\pm\pi$), these additional intersection points are always of a suboptimal nature and do not affect the differentiability of V. We have yet to understand how and where the curves of intersection points end as the holes around $\pm\pi$ close.

The complete suboptimal solution set up to level 10.89 is shown in Figure 7. When viewed along the negative V-axis, the graph of this multi-valued function is identical to that in Figure 4. Each self-intersecting level set still has only 4 intersections, but as an object things look much more complicated. Nevertheless, from a geometrical point of view, one can imagine that this object must be smooth when lifted into some higher-dimensional space. This will be explained in more detail in the next section.

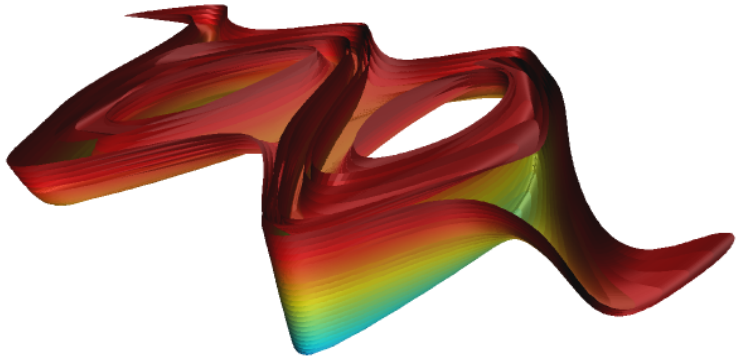

Figure 7: *The suboptimal level sets of the multi-valued function associated with V up to* 10.89. *The color coding is as in Figure 3. When viewed along the negative V-axis this object is the same as in Figure 4; see also the animation in the multimedia supplement [Osinga and Hauser, 2005].*

5 Variational methods: Pontryagin's Minimum Principle

The second approach to solving optimal control problems is via the use of Lagrange multipliers. Pontryagin's Minimum Principle is, in effect, a clever interpretation of the Euler-Lagrange equation in variational calculus; see [Pontryagin *et al.*, 1962], [Sussmann and Willems, 1997] and [Sussmann, 1998]. Namely, we seek to minimize the functional

$$\int_0^\infty q(x(t), u(t))\, dt$$

over pairs $(x(t), u(t))$ that satisfy $\dot{x} = f(x, u)$. The main idea is to introduce a time-dependent Lagrange multiplier $p = p(t)$ and consider the pre-Hamiltonian (4)

$$K(x, p, u) = q(x, u) + p^T f(x, u).$$

Recall that we assumed the existence of a C^1 map $u^* = u^*(x, p)$ that globally minimizes $K(x, p, u)$. At this critical point $u = u^*$ we obtain the Hamiltonian

$$H(x, p) := K(x, p, u^*(x, p)) = q(x, u^*(x, p)) + p^T f(x, u^*(x, p)) \tag{9}$$

that is related to the original problem and the associated Euler-Lagrange equation via a Legendre transformation; see [Sontag, 1998], [Sussmann and Willems, 1997] and [Sussmann, 1998]. Pontryagin's Minimum Principle says that if the pair $(x_0, u^*(\cdot))$ is optimal, then the optimal trajectory pair $(x^{u^*}(\cdot), u^*(\cdot))$ corresponds to a trajectory $(x^*(\cdot), p^*(\cdot))$ via $u^*(t) = u^*(x^*(t), p^*(t))$ along which $H(x,p)$ is constant. Hence, $(x^*(\cdot), p^*(\cdot))$ is a solution to the Hamiltonian system

$$\left\{ \begin{array}{rcl} \dot{x} &=& \dfrac{\partial}{\partial p} H(x,p) \;=\; f(x,u^*), \\ \dot{p} &=& -\dfrac{\partial}{\partial x} H(x,p). \end{array} \right.$$

Furthermore, $(x^*(\cdot), p^*(\cdot))$ lies on the stable manifold $W^s(0,0)$ of the origin, since $(x^*(t), p^*(t)) \to (0,0)$ as $t \to \infty$; see [Van der Schaft, 2000, chapter 8].

Van der Schaft [2000] showed that the origin of this Hamiltonian system is a saddle with no eigenvalues on the imaginary axis. The stable eigenspace $E^s(0,0)$ is spanned by

$$E^s(0,0) = \text{span} \left[\begin{array}{c} I_n \\ 2P \end{array} \right],$$

where P is the solution of the algebraic Riccati equation (7). For the linearized problem, this means that the value function V_L is implicitly present in the Hamiltonian system as the Lagrangian of the stable manifold, that is, trajectories on the stable manifold satisfy

$$H(x,p) = H\left(x, \nabla V_L^T(x)\right) = 0.$$

Locally, we can immediately see that a Lagrangian V exists for the nonlinear problem as well. Namely, we know from the Stable Manifold Theorem that $W^s(0,0)$ is tangent to $E^s(0,0)$; see [Palis and de Melo, 1982]. Van der Schaft uses this to generalize the existence, uniqueness, and smoothness results to the nonlinear case. His results hold for the local stable manifold $W^s_{\text{loc}}(0,0)$, which is Lagrangian and associated with a sufficiently small neighborhood of the origin in the original state space of the problem.

The result can be interpreted as follows. For a given initial condition $x = x_0$, one obtains the optimal control and associated optimal cost by finding $p := p_0$ such that the point (x_0, p_0) lies on $W^s(0,0)$. Locally near the origin, where $W^s(0,0)$ can be viewed as the graph of a function $x \mapsto p = \nabla V^T(x)$, the choice for p_0 is unique. When $W^s(0,0)$ starts to fold back over itself with respect to the x-space,

there are more than one possible choice for p_0. However, for most choices, the associated optimal cost is only locally optimal and the associated solution is not the required globally minimal solution. In [Hauser and Osinga, 2001] it is shown that the projection of $W^s(0,0)$ onto the x-space entirely covers the stabilizable domain for nonlinear control problems of the class described in Section 2.1. This means that all initial conditions $x = x_0$ that can be driven to the origin have at least one associated value p_0 for p such that $(x_0, p_0) \in W^s(0,0)$.

For the example of the balanced pendulum we obtain a four-dimensional associated Hamiltonian system. Since the (original) vector field is affine in the control u, we can explicitly write down $u^*(x,p)$ that minimizes the pre-Hamiltionian:

$$u^*\left(\begin{bmatrix} x_1 \\ x_2 \end{bmatrix}, \begin{bmatrix} p_1 \\ p_2 \end{bmatrix}\right) = -\frac{1}{r_1}\begin{bmatrix} 0 & \frac{\frac{m_r}{ml}\cos(x_1)}{\frac{4}{3} - m_r\cos^2(x_1)} \end{bmatrix}\begin{bmatrix} p_1 \\ p_2 \end{bmatrix}.$$

The Hamiltonian now follows immediately from Eq. (9).

Computing a two-dimensional global invariant manifold such as $W^s(0,0)$ is a serious challenge; see [Krauskopf *et al.*, 2005] for an overview of recently developed techniques. We computed (a first part of) $W^s(0,0)$ with the algorithm described in [Krauskopf and Osinga, 2003]. In these computations, we focus solely on the dynamical system defined by the Hamiltonian (9), and ignore the associated optimal control problem, including the value of the cost involved in (locally) optimally controlling the system. The algorithm computes *geodesic level sets* of points that lie at the same geodesic distance to the origin. This means that the manifold is growing uniformly in all (geodesic) radial directions; we refer to [Krauskopf and Osinga, 2003] for more details. Projections of $W^s(0,0)$ are shown in Figure 8. The alternating dark and light blue bands indicate the location of the computed geodesic level sets. Animations of how the manifold is grown can be found in the multimedia supplement [Osinga and Hauser, 2005].

Figure 8(a) shows the vertical projection of $W^s(0,0)$ onto the (x_1, x_2)-plane such that it can be compared with Figure 3. For convenience Figure 3 is reproduced here as Figure 8(b). Note that $W^s(0,0)$ is an unbounded manifold, even though it seems to be bounded in some of the x_1- and x_2-directions in a neighborhood of the origin. In this neighborhood, the manifold stretches mainly in the p_1- and p_2-directions. A better impression of the manifold is given in Figures 8(c)-(d), where the manifold is projected onto a three-dimensional space; Figure 8(c) shows the projection $\{p_2 = 0\}$ and Figure 8(d) the projection $\{p_1 = 0\}$. In each figure the manifold is only rotated away slightly from its position in Figure 8(a). A sense of depth is also given by considering the rings near the origin, which are almost perfect circles in $\mathbb{R}^4$ because the manifold is very flat initially. The distortion of

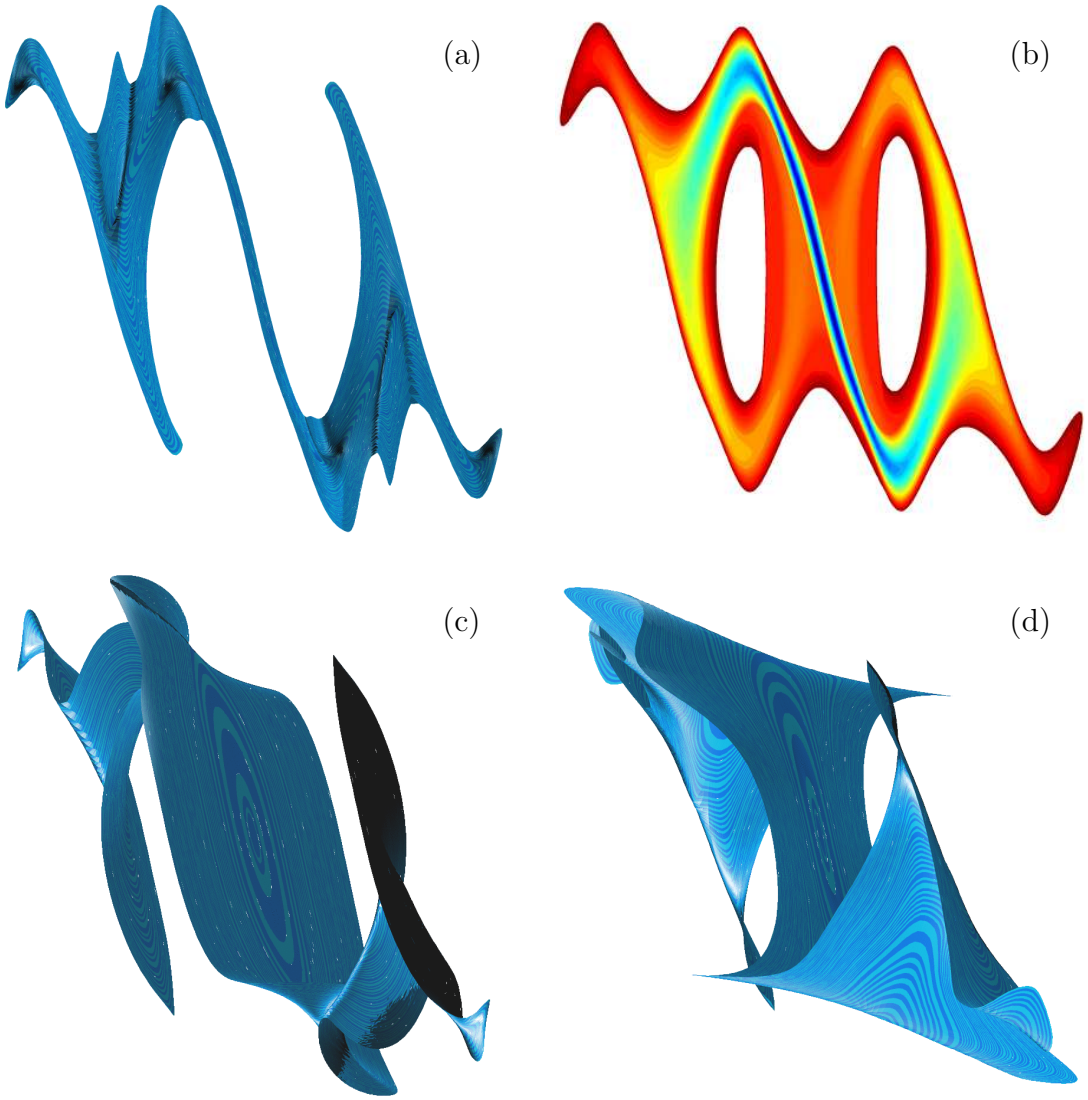

Figure 8: *The stable manifold $W^s(0)$ associated with the Hamiltonian (9) (panel a) is directly related to the value function V (panel b) as can be seen in the projection onto the $(x1, x2)$-plane. This manifold lives in a four-dimensional space and three-dimensional projections are shown as rotations in (x_1, x_2, p_1)-space (panel c) and (x_1, x_2, p_2)-space (panel d); see also the animation in the multimedia supplement [Osinga and Hauser, 2005].*

these circles in Figures 8(c)-(d) is due to the viewpoint of the projections. The animations in the multimedia supplement [Osinga and Hauser, 2005] give a better idea of what $W^s(0,0)$ looks like in four-dimensional space.

6 Singularities of the value function

While the approach using dynamic programming directly leads to the value function V, this function is intrinsically present in the Hamiltonian formulation. As mentioned in the previous section, the local stable manifold $W^s_{\rm loc}(0,0)$ is Lagrangian and can be viewed as the graph of a function $x \mapsto p = \nabla V^T(x)$. We can extend the definition of V outside this neighborhood of the origin if we allow V to be a multi-valued function. That is, by including suboptimal solutions V is defined everywhere on $W^s(0,0)$. Moreover, as a function of (x,p), the value function V is C^1 everywhere, because the cost function $q(x,u)$ is C^2 and the (sub)optimal solutions follow a C^2 path along $W^s(0,0)$.

Effectively, we lift the graph $(x,V(x))$ into a higher-dimensional space such that it becomes a smooth manifold. That is, we enlarge the domain such that the multi-valued function $x \mapsto V(x)$ becomes a well-defined single-valued function $(x,p) \mapsto V(x,p)$ that is equal to (sub)optimal values of the total cost for all points $(x,p) \in W^s(0,0)$. Since $W^s(0,0)$ is as smooth as the vector field, this subset of $V(x,p)$ forms a C^1 manifold.

After the transformation into (x,p)-space *all* level sets of V are smooth topological circles, not only the ones up to $V = 6$ where V is a well-defined function. It is not easy to visualize this, since the transformed level sets should be viewed in $\mathbb{R}^4$. However, an impression is given in Figure 9. Figures 9(a) and (b) show the level sets for $V = 3.24$ and $V = 6.8644$ in $\mathbb{R}^2$ as in Figures 6(a) and (c). Their transformations into $\mathbb{R}^4$ are shown in Figure 9(c) together with $W^s(0,0)$. The chosen view point involves all four directions in $\mathbb{R}^4$ and the self-intersections of the level set $V = 6.8644$ in this lift are now due to projection. Note that the level sets are computed using dynamic programming combined with continuation techniques to pick up the suboptimal solutions. The stable manifold $W^s(0,0)$ is computed using the algorithm of [Krauskopf and Osinga, 2003]. Neither method preserves the symplectic structure that ensures the Hamiltonian (9) remains constant (at zero). This slight numerical discrepancy is the likely reason why the level sets do not lie exactly on the surface of $W^s(0,0)$. However, the numerical approximation of $W^s(0,0)$ does show well that the value function is smooth in this Hamiltonian setting.

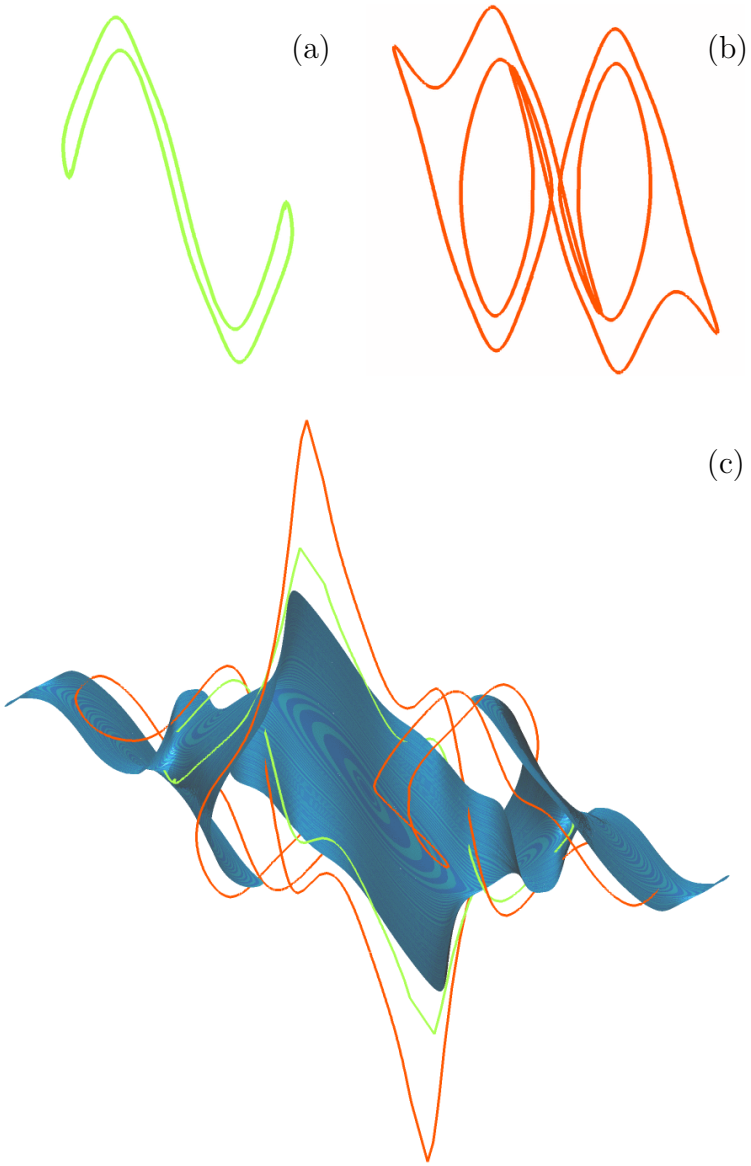

Figure 9: *Two (locally) optimal level sets of the multi-valued function V, one for $V = 3.24$ (a) and one for $V = 6.8644$ (b) in $\mathbb{R}^2$ and their transformations into (x, p)-space together with the stable manifold $W^s(0, 0)$ (c).*

7 Summary of results

Dynamic programming is often viewed as the approach leading to an optimal control strategy in feedback form. In order to obtain such solutions, many restrictions need to be imposed on the system and the theory only provides *sufficient* conditions for optimality of solutions. On the other hand, variational methods provide solutions from which the optimal control strategy is not easily extracted. This theory needs far fewer restrictions and *necessary* conditions are obtained.

Using Pontryagin's Minimum Principle, we reformulated the optimal control problem into the problem of finding the stable manifold of the origin in a Hamiltonian system. The necessary conditions that lead to the stable manifold $W^s(0,0)$ of the Hamiltonian system are sufficient to show global existence of the value function V on the stabilizable domain. Note that global existence of V is often imposed as a condition; see for example [Van der Schaft, 2000]. The existence of V, however, directly follows from the fact that $W^s(0,0)$, when projected onto the x-space, covers the stabilizable domain; compare with [Day, 1998] where global existence of V is shown by imposing the condition that the projection of $W^s(0,0)$ onto the state space covers the stabilizable domain.

The solutions of the variational method also lead to an optimal control strategy in feedback form via the transformation back to the control setting. All extremal solution pairs $(x_0, u^*(\cdot))$ directly transform to trajectories on $W^s(0,0)$ and we have the following diagram:

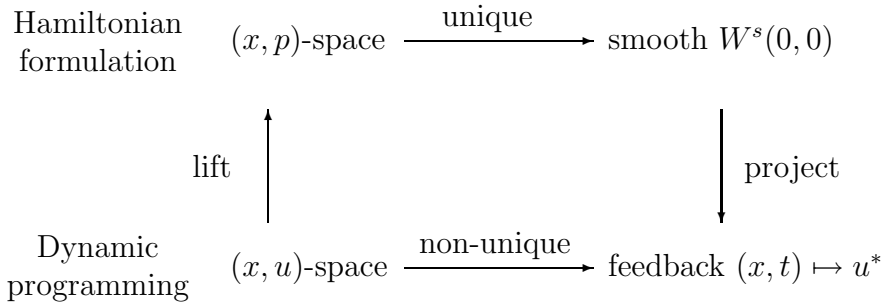

As illustrated with the simple example of balancing a pendulum on a moving cart, the two approaches go hand-in-hand for the general class of systems introduced in Section 2.1.

Acknowledgments

We gratefully acknowledge fruitful discussions with Chris Byrnes, Francis Clarke, Arthur Krener, and Arjan van der Schaft. Special thanks go to Bernd Krauskopf for his helpful comments on an earlier version of this paper. The research was supported by AFOSR/DDRE MURI AFS-5X-F496209610471, and we thank California Institute of Technology for its hospitality.

References

Bardi, M., and Capuzzo-Dolcetta, I. (1997). *Optimal Control and Viscosity Solugions of Hamilton Jacobi Bellman Equations*, Birkhäuser, Boston.

Buttazzo, G., Giaquinta, M., and Hildebrandt, S. (1998). *One-Dimensional Variational Problems*, Oxford University Press, New York.

Cesari, L. (1983). *Optimization — Theory and Applications: Problems with Ordinary Differential Equations*, Springer-Verlag, New York.

Dacorogna, B. (1989). *Direct Methods in the Calculus of Variations*, Springer-Verlag, New York.

Day, M.V. (1998). On Lagrange manifolds and viscosity solutions. *J. Math. Systems, Estimation and Control* **8**(3), 369–372.

Hauser, J., and Osinga, H.M. (2001). On the geometry of optimal control: the inverted pendulum example. In Proc. Amer. Control Conf., Arlington VA, June 25–27, pp. 1721–1726.

Jadbabaie, A., Yu, J., and Hauser, J. (1999). Unconstrained receding horizon control: Stability region of attraction results. In Proc. Conf. on Decision and Control, # CDC99-REG0545.

Jadbabaie, A., Yu, J., and Hauser, J. (2001). Unconstrained receding horizon control of nonlinear systems, *IEEE Trans. Automatic Control* **46**(5), 776–783.

Krauskopf, B., and Osinga, H.M. (2003). Computing geodesic level sets on global (un)stable manifolds of vector fields, *SIAM J. Appl. Dyn. Sys.* **2**(4), 546–569.

Krauskopf, B., Osinga, H.M., Doedel, E.J., Henderson, M.E., Guckenheimer, J., Vladimirsky, A., Dellnitz, M., and Junge, O. (2005). A survey of methods for computing (un)stable manifolds of vector fields, *Int. J. Bifurcation and Chaos* **15**(3), 763–791.

Lee, E.B., and Markus, L. (1967). *Optimization—Theory and Applications: Problems with Ordinary Differential Equations*, John Wiley & Sons, New York.

Lukes, D.L. (1969). Optimal regulation of nonlinear dynamical systems, *SIAM J. Control* **7**(1), 75–100.

Osinga, H.M., and Hauser, J. (2005). Multimedia supplement with this paper; available at `http://www.enm.bris.ac.uk/anm/preprints/2005r28.html`.

Palis, J., and de Melo, W. (1982). *Geometric Theory of Dynamical Systems*, Springer-Verlag, New York.

Pontryagin, L.S., Boltyanski, V.G., Gamkrelidze, R.V., and Mischenko, E.F. (1962). *The Mathematical Theory of Optimal Processes*, John Wiley & Sons, New York.

Schaft, A.J. van der (2000). *L_2-Gain and Passivity Techniques in Nonlinear Control*, Springer-Verlag, New York, 2nd edition.

Sontag, E.D. (1998). *Mathematical Control Theory: Deterministic Finite Dimensional Systems*, Texts in Applied Mathematics 6, Springer-Verlag, New York, 2nd edition.

Sussmann, H.J., and Willems, J.C. (1997). 300 years of optimal control: From the brachystochrone to the maximum principle, *IEEE Control Systems Magazine* June issue, 32–44.

Sussmann, H.J. (1998). Geometry and optimal control. In Baillieul, J. and Willems, J.C. (eds.), *Mathematical Control Theory*, Springer-Verlag, New York, pp. 140–198.